CLM-R277

CLM-R277

A High Power CO_2 Laser Beam Monitor and Instrumentation for Laser Processing System Operators

A.J.B. Travis

UK ATOMIC ENERGY AUTHORITY

Culham Laboratory

A High Power CO_2 Laser Beam Monitor and Instrumentation for Laser Processing System Operators

A. J. B. Travis
UKAEA Culham Laboratory, Abingdon, Oxon, OX14 3DB, UK

ABSTRACT

A monitor is described that can be used routinely by the operator of a high power CO_2 laser being used for material processing to measure and record a number of the beam characteristics of the laser.

The microprocessor controlled monitor gathers data from a low powered sample of the laser beam. The monitor measures the power transmitted through a wavelength sensitive element, polarisation analysers and variously shaped and sized pinholes which have been positioned precisely over an image of the far field intensity profile of the laser beam. The parameters monitored are: the shape and stability of the far field intensity profile; plane of polarisation; divergence; pointing stability, and wavelength fluctuations. Data can be reduced to give beam quality assurance, and presented in a detailed form either for recording as part of quality assurance documentation or for use by laser maintenance personnel. Monitor control is by colour coded switches and menus, and requires a minimum of operator involvement or training.

Culham Laboratory
United Kingdom Atomic Energy Authority
Abingdon
Oxfordshire OX14 3DB

June 1987

Amendment to CLM-R277
The *correct* ISBN number should read:

ISBN: 085311 160X
C.18
Price: £5.00
Available from H. M. Stationery Office

1. INTRODUCTION

The quality of CO_2 laser machining processes, for example cutting, heat treatment or welding, depends upon a number of parameters such as workpiece consistency and handling methods, laser beam handling and focusing, gas shroud and jets, and the characteristics of the laser output beam[1]. During process development, these parameters are optimised to give the best product. The reproducibility of the process is dependent upon the ability to produce and maintain these optimised parameters within pre-determined tolerance limits[2]. The current work to monitor the characteristics of a CO_2 laser output beam is part of a larger programme to identify the more crucial factors in laser machining which exhibit a non-linear or discontinuous influence on the product. Recent studies have highlighted some laser-stability requirements[3] and analysed the possible physical and technical reasons for fluctuations in the power and spatial distribution of a laser beam[4].

The beam parameters may be divided into two categories. Those which determine the amount and distribution of the laser's power falling on the workpiece, and the coupling efficiency of this power into the workpiece surface.

A power monitor is the most common, and in many cases, the only diagnostic apparatus normally included as standard in a commercially available laser package. However, because of the possibility of the laser developing highly divergent wall modes or of changes in the transmittance of the beam delivery system, power monitors do not always accurately reflect the amount of power actually falling on the workpiece.

The most commonly observed power fluctuation is that caused by the longitudinal mode variations. The absence of these is sometimes interpreted as a sign of a very stable cavity. However, observations of the longitudinal and transverse mode beat frequencies[5] of a laser which lacked any discernable longitudinal mode power fluctuations showed activity in both the longitudinal and transverse modes, indicating that the power stability was associated with multi mode operation.

The shape of the intensity profile and the power distribution on the workpiece surface is generally acknowledged to be an important factor in

determining the effectiveness with which the incident power is coupled into the process. The majority of CO_2 laser processing systems focus the laser beam onto the surface of the workpiece to obtain a smaller area of higher intensity radiation. The intensity profile in the focal plane of a perfect lens is the same shape as the far field intensity profile of the laser beam.

Observations on a number of lasers have shown that the far field intensity profile is subject to both slow and fast fluctuations. The slow fluctuations occur over periods of greater than one second. Cyclic variations in the peak intensity of up to ±10% have been observed in synchronism with the longitudinal mode power fluctuations. Other slow variations can be caused by changes in the cavity alignment and to variations in the laser's operating conditions such as cooling water temperature. These variations can be observed if intensity profile data is plotted over a period of a few days. The fast fluctuations have a frequency above 1Hz, and can exceed ±20%. The frequency spectrum of these fluctuations (usually in the range 1Hz-1kHz) can be related to the spectrum of vibration of the laser, power supply ripple and flow turbulence. The fast fluctuations can be associated with wavelength jumps from the normal 10.4μm band to the associated 9.4μm band, and with large changes in the apparent plane of polarisation. There is some evidence from our work that variations in the plane of polarisation can also be associated with the longitudinal mode variations. Fluctuations of the plane of polarisation and of wavelength have also been observed by V.A. Dymshakov et al[6].

The focal spot size varies with wavelength and the quality of a cut depends upon the plane of polarisation at the surface[7,8]. Polarisation changes have also been observed during machining operations, and these are thought to be caused by reflections from the workpiece coupling into the laser's cavity[9]. If these reflections are decoupled using 1/4 wave retarders, deterioration of these elements with time can be monitored by observing the ellipticity of the polarisation of the beam.

Other parameters which can affect the coupling of the laser power into the workpiece are the beam divergence and pointing stability, since these in turn affect the intensity profiles and spot position produced

by any beam focusing elements. The timescales of variations in these parameters are normally greater than a minute. Divergence is sensitive to the ageing and replacement of the laser cavity optical components. The beam pointing stability can be affected by changes in the laser cavity alignment, and may vary considerably in the period immediately after laser start up.

A number of CO_2 laser beam monitoring techniques have been described and assessed[10,11,12,13,14], and others are now becoming commercially available. Each of these instruments only monitors some of the above areas of interest, and many, in their presently available form, are orientated towards laboratory use rather than general continuous and easy use in an industrial environment.

The most recent part of the work described here has been the development of a laser beam monitor for use by a process operator. This is a monitor that can be used routinely by the operator of a laser processing system to observe a range of the laser's output beam characteristics. It is able to provide the process control logic with a quality assurance signal. The software provided with the monitor is also capable of presenting the descriptive parameters of a beam in a more detailed manner for recording as part of quality assurance documentation and for use by laser maintenance personnel.

The laser beam parameters that can be monitored by the instrument are as follows:-

- Far field intensity profile fluctuations.
- Far field power distribution fluctuations.
- Polarisation ellipticity.
- Wavelength fluctuations.
- Divergence fluctuations.
- Beam pointing direction.
- Longitudinal and transverse mode beating.
- Laser beam power at the monitor position.

To fulfil its role in an industrial environment, the monitor has been designed to:-

- Monitor multi-kilowatt CO_2 laser beam parameters, both during and between machining operations.

- Be robust and basically simple in concept and construction.
- Be simple to operate and require very little operator training.
- provide simplified data for a process control system and/or operator for quality assurance of the laser output beam.
- Provide comprehensive quantitative monitoring of the laser beam for storage as part of the overall product quality control strategy, and to assist maintenance personnel in fault identification and rectification.
- Give advance warning of possible laser malfunctions or accelerated component ageing to allow corrective measures to be taken during routine maintenance periods.
- Assist readjustment of the laser after routine maintenance or breakdown.
- Characterise a new laser as part of acceptance trials.

2. DESCRIPTION OF THE LASER BEAM MONITOR

A schematic diagram of the monitor system, together with the method of insertion into the beam delivery line is shown in Fig. 1. The laser beam is sampled using a partially transmitting element to allow monitoring during machining operations. Under normal working conditions the internal laser beam shutter remains open. Delivery of the laser beam to the workpiece is controlled by a supplementary shutter inserted after the monitor system.

2.1 Beam Sampling and Far Field Image Production Assembly

Beam sampling is performed by a hole matrix mirror, this being a mirror having a matrix of small transmitting holes[15]. The fraction of the beam transmitted by this element forms a matrix of images of the far field intensity profile of the incident beam in the focal plane of an imaging lens placed behind the hole matrix mirror. An example of the burn pattern made by such a matrix of far field images in an acrylic target is shown in Fig. 2. The central far field image is initially centred within the monitor assembly input aperture using the pre-alignment mirror and telescope (Fig. 1), and the beam from the alignment HeNe Laser fitted to the CO_2 laser. The beam sampling and image production parameters are given in Table 1.

2.2 Monitor Assembly

A schematic diagram of the monitor assembly is shown in Fig. 3 and a general view in Fig. 4. With reference to Fig. 3, the plane of the pinhole disc is set to be coincident with the far field image plane (Fig. 1). The disc is mounted on the shaft of a stepper motor[16]. On the disc are mounted a number of different sized pinholes, any of which can be positioned in front of the detector by suitable rotation of the disc. The pinhole disc latch ensures accurate and reproduceable co-axial alignment of the selected pinhole with the detector. The detector measures the amount of power transmitted through the selected pinhole. Two interchangeable detectors are available. The first is a pyroelectric detector[17]. This is used to measure the power passing through the pinholes and also the amplitude of any laser fluctuations up to a frequency of 1kHz. A schematic diagram of the associated electronics is shown in Fig. 5a. The second detector is a room temperature HgCdTe photoconductor[18] and is used to monitor longitudinal and transverse mode beating activity[5] in the range 0.1→50MHz. A schematic diagram of the associated electronics is shown in Fig. 5b. The electronic filter units transmit only the longitudinal or the transverse mode beat frequencies. The pinhole and detector assemblies (Fig. 3) are mounted on a stepping motor driven X-Y positioning assembly[19] which allows indexed alignment of the pinhole/detector axis with the central image of the far field image array. A six position disc assembly, the attenuator disc, is positioned in front of the pinhole disc. The items mounted on the pinhole and attenuator discs are summarised in Tables 2 and 3.

2.3 Monitor Control, Data Acquisition and Analysis

The monitor is controlled by a microprocessor for routine acquisitions of data. Two modes of operation are available, both for use with the pyroelectric detector. The required mode is selected using simple colour coded menus and switches.

The first mode of operation employs a software routine which results in the accurate alignment of the pinhole/detector axes with the maximum intensity of the previously selected central far field image. Under the control of the software, the motorised X-Y positioning assembly moves the pinhole/detector assembly around an 11 x 11 square array of sampling points. At each sampling point the detector output signal is recorded.

The initial array has the length of its sides equal to the space between far field images. The pinhole/detector assembly is then moved to the array position giving the maximum detector output. Repeating this procedure using arrays having successively smaller sides allows a progressive improvement in alignment. The data from this process can be output to a line printer (Fig. 6a). The detector output signals are normalised and rounded to the nearest hexadecimal value to produce a more easily interpreted display. This array of detector output signals can be further processed by another computer to produce visual representations of the circular symmetry of the intensity profiles (Fig. 7).

The second mode of operation employs a software routine to provide information pertinent to the far field intensity profile and its fluctuations, plane of polarization, wavelength and divergence variations, and power. This routine is normally only entered after the alignment mode has been completed. The software interprets the detector signal associated with eleven combinations of pinhole and attenuator disc positions. For each combination, 16 values of detector output are recorded. These are processed, displayed, and printed as shown in Fig. 6b. The third column of this output gives the mean of the 16 values associated with the indicated pinhole/attenuator combination, expressed as a percentage of the mean signal obtained from the 3.2mm square pinhole combination. Column four is the root mean square of the 16 values expressed as a percentage of the mean. The fifth column lists the average intensities in each of the annuli defined by successive pinhole radii.

The monitor system can be operated in a manual mode to assist in laser system maintenance. The detector outputs in this case are displayed on suitable additional equipment.

3. RESULTS AND DISCUSSION

The primary function of a laser beam monitor is to give beam quality assurance, i.e. that the present beam parameters are within previously determined process tolerance limits. All the lasers currently observed exhibit different beam parameters, some of which vary with time within definable limits. These normal variations must be less than the process tolerance limits. Advance warning of a possible laser malfunction

occurs when the laser shows variations which are outside its own characteristic limits, but still within the process tolerances. Details of the quantitative information which can be obtained from the monitor are given in the Appendix.

The normal mode of operation is with the pyroelectric detector installed. After the initial alignment using the first mode of operation, the matrix step size is set to 40μm. Full sets of data (Fig. 6) can then be gathered on demand, the minimum cycle times being 35s for routine 1 and 90s for routine 2.

The position co-ordinates of the maximum output signal from the pyroelectric detector (Fig. 6a) are an indication of the beam pointing direction. Observation of the movement of this point permit an estimate to be made of the stability of the combined beam pointing and beam delivery system alignment. The array step size and the position co-ordinates are recorded in micrometers.

The 100% TRANS. DETECTOR OUTPUT at the top of Fig. 6b represents the total power contained in one of the far field images, and is proportional to the laser power falling on the hole matrix mirror. This signal is therefore an "on line" total beam power monitor.

The first nine lines of the table of data (Fig. 6b) give information about the far field profiles and their stability. When compared with previous data they will show up any abnormal variation in the laser's long term performance. Fig. 8 shows intensity distribution values (Fig. 6b, Col 5) for a fast axial flow laser recorded over a period of six days. The large fluctuations on day 6, indicating unacceptable conditions at the workpiece, were not due to laser malfunctions, but caused by the accidental contamination of the atmosphere in the laser beam delivery line. The values listed in column 4 of Fig. 6b are estimates of the R.M.S. value of the fast fluctuations (5Hz - 1kHz) in specific areas of the far field intensity profile. An example of the output signal from the pyroelectric detector which shows these fast fluctuations is shown in Fig. 9. An increase in the amplitude of these fluctuations can be a warning of potential laser malfunction[4]. Examples of the different characteristics exhibited by different types of laser is given in Fig. 10. The divergence of the laser beams can be

monitored and compared by measuring the diameter which contains 86.5% ($1-1/e^2$) of the beam power. Absolute values of the average intensities in the annuli (Fig. 6b) together with the associated transmissions are given in Fig. 11. The profiles in Fig. 10 together with the derived data display from sequence No. 1 (Fig. 7) give a good visual indication of the far field intensity and power distribution profiles.

Lines 10 and 11 of the table in Fig. 6b give information about the polarisation of the beam. The transmissions (col 3) through the two orthogonally orientated grid polarisers can be interpreted to indicate the direction of the effective plane of polarisation of the beam. (Allowance must be made for the transmission coefficient of the grid polarisers.) The R.M.S. values (col 4) indicate the degree of fluctuation of this plane of polarisation. An example of the output signal from the pyroelectric detector when the laser's polarisation stability is being effected by large vibrations of the laser cavity components is shown in Fig. 12.

Line 12 of the table (Fig. 6b) gives information about the wavelength stability of the laser. The transmission (col 3) of the CaF_2 disc can be interpreted (in the absence of power fluctuations) to give an indication of the wavelength(s) at which the laser is operating. The variation of transmission with wavelength of this disc is shown in Fig. 13. An example of the form of the detector output signal associated with wavelength changes is shown in Fig. 14.

When operating the monitor with the photoresistive detector installed, (see Section 2.2) the monitor is normally under manual control with the 3.2mm square pinhole selected. Fig. 15 shows an example of the variation of longitudinal and transverse mode beat frequency amplitude over a longitudinal mode cycle. Zero amplitude (Fig. 15) is obtained when only a single longitudinal and transverse mode is present. The presence of a second mode produces a detectable and specific beat frequency. Although the ratio of the mode amplitudes cannot be readily quantified from the amplitude of the beat frequency without the use of a suitable local oscillator, the information provided will readily detect cavity misalignments and any changes from single to multi-mode operation which may be caused by cavity component replacement.

4. CONCLUSIONS

The accumulation of experience with laser machining processes has highlighted the necessity for an easily operable monitor which can record the laser beam characteristics during machining processes. This information is particularly important when process repeatability is paramount, such as in the nuclear industry, when processing expensive components, or where the quality of a product is being improved for commercial reasons.

A monitor for this purpose has been defined and constructed, the design specification being based upon the present understanding of laser/workpiece interactions. The monitor design is mechanically simple, and the incorporation of a microprocessor ensures ease of operation and data interpretation.

The structure of the data analysis software enables the monitor to display and store a comprehensive range of information and also to compress this information into a simple laser beam quality assurance signal for transmission to process control equipment.

The observation that different makes of laser exhibit a subtly different range of output beam characteristics, each of which may be advantageous or disadvantageous to a particular machining operation, introduces another constraint on the choice of laser for a particular process.

5. ACKNOWLEDGEMENTS

This work was performed on behalf of the Northern Division of the UKAEA and the author gratefully acknowledges their support and encouragement. The author would also like to thank BA Ward for his advice and guidance, and SP Walde for his considerable assistance in writing the control and analysis software.

6. REFERENCES

(1) J Fieret, MJ Terry, BA Ward, preprint CLM-P780, UKAEA Culham Laboratory, Abingdon, Oxon (1986).

(2) MK Burris, Technical Communication BDX-613-2497, The Bendix Corporation, Kansas City Division, PO Box 1159, Kansas City, Missouri 64141, (1980).

(3) IJ Spalding, Sixth International Symposium on Gas Flow & Chemical Lasers, Jerusalem, 8-12 September 1986.

(4) VS Golubev, FV Lebedev, Sov. J. Quantum Electron. 15(4), April 1985, pp437-442.

(5) PV Gatenby, KC Hawkins, HN Rutt, J. Phys. E: Sci Instrum., Vol. 14, 1981, pp56-57.

(6) VA Dymshakov, FV Lebedev, AV Ryazanov, Sov. J. Quantum Electron. 15(2), Feb 1985, pp195-198.

(7) FO Olsen, Proc. A.S.D. Conf. Applications of Lasers in Material Processing, Los Angeles, Jan 1983.

(8) SE Nielsen, Phd Thesis, Inst. Manfg. Eng., Technical University of Denmark, 1985.

(9) TA Jones, CE Albright, Applied Optics, Vol. 23, No. 13, July 1984, pp2065-2069.

(10) RC Crafer, PJ Oakley, Research Report 165/1981, The Welding Inst., Cambridge (1981).

(11) BA Ward, published in Proc. of Second Symp. on Exploiting the Laser in Engineering Production, Coventry, 18-19 Sept, 1984, The Welding Inst.

(12) GC Lim, WM Steen, Opt. Laser Tec., p149, June 1982.

(13) IW Boyd, JG Crowder, J. Phys. E: Sci. Instrum., 15, p421, 1982.

(14) AJB Travis, Preprint CLM-P751, Culham Laboratory (1984).

(15) E Harvey, HL Scott, Opt. Eng. Vol. 20, No. 6, Dec 1981, pp881-886.

(16) M Calderon Ltd, London EC1.

(17) Molectron Corp., Sunnyvale, CA94086.

(18) Radec, Institute of Plasma Physics and Laser Microfusion, Warsaw, Poland.

(19) Oriel Scientific Ltd, PO Box 136, Kingston Upon Thames, Surrey KT1 1QU.

(20) Cambridge Physical Sciences, Milton Road, Cambridge CB4 4DW.

(21) Analytical Accessories Ltd, Unit 3, Lagoon Road, St Mary Cray, Orpington, Kent BR5 3QX.

TABLE 1

Beam Sampling and Far Field Image Production Parameters

Hole Matrix	
Incident beam angle of incidence	45°
Hole diameter	0.3mm
Hole counterbore diameters	2.5mm
Hole spacing	3.0mm
Matrix size	17 x 17
Imaging Lens	
Focal length	1 metre
Lens material	ZnSe
Far Field Image Separation	3.2mm

TABLE 2

Pinhole Disc Component Positions

Disc Position	Component
1	0.3mm$_\phi$ pinhole
2	0.6 "
3	1.0 "
4	1.5 "
5	2.0 "
7	2.5 "
8	3.0 "
9	3.2mm square aperture

TABLE 3

Attenuator Disc Component Positions

Disc Position	Component
1	18mm aperture
2	Grid Polariser (orientation 90°)[20]
3	Alignment target
4	Grid Polariser (orientation 0°)[20]
5	18mm aperture
6	4mm thick CaF_2[21]

Appendix

Quantitative Interpretation of Monitor Output Data

Calibration of Pyroelectric Detector

With reference to Fig. 5a the gain of amplifier 1 is set to the reciprocal of the laser power (in kilowatts) falling on the hole matrix. The gain (G) of the microprocessor controlled amplifier 3 is set to unity. The gain of amplifier 2 is then set so that with the 3.2mm square pinhole in front of the detector the microprocessor records 1000 units of power.

The pyroelectric detector is normally operated with the gain of amplifier 1 set to the reciprocal of the laser's average output power (P_I kilowatts) shown by the internal power meter of the laser.

Pyroelectric Detector with Data Acquisition Sequence No. 1

Referring to Fig. 6a the position of the imaging lens (Fig. 1) is initially set to give a maximum recorded value of the detector output (DET O/P). (This value is the maximum detector signal observed during the matrix scan). If the beam pointing direction changes with time the peak of the far-field image will move within the matrix of sampling points, and the matrix position will be moved to compensate. However, the peak position co-ordinates (in μm) are always given relative to the initial position of the centre of the scan matrix. The variations in these peak position co-ordinates (δx, δy) are directly related to variations in beam pointing ($\delta\theta_x$; $\delta\theta_y$) by the relationships

$$\delta\theta_x = \frac{\delta x}{f} \qquad (1)$$

$$\delta\theta_y = \frac{\delta y}{f} \qquad (2)$$

where f is the distance of the image plane from the imaging lens.

Pyroelectric Detector with Data Acquisition Sequence No. 2

This sequence is normally run only after the maximum of the far-field image has been aligned with the pinhole/detector axis using sequence No 1. In Fig. 6b, the 100% TRANS. DETECTOR OUTPUT (D_{100}) is the detector signal associated with the 3.2mm square pinhole. This is

related to the power falling on the hole matrix (P_m) by:

$$P_m = D_{100} P_I \text{ watts} \quad (3)$$

The transmissions and average intensities in the annuli (Fig. 6b) are indicated in Fig. 11. The printout units of intensity (I_p) are power units/mm^2 and are converted to intensity (I_m) by the relationship:

$$I_m = 100(I_p P_I) \text{ watts/cm}^2 \quad (4)$$

These values of intensity can be related to those on the workpiece (I_w) by:

$$I_w = I_m \, T\left(\frac{F_m^2}{F_w}\right) \text{ watts/cm}^2 \quad (5)$$

where F_m and F_w are the effective optical aperture F numbers of the monitor and workpiece imaging systems and T is the transmission of the beam delivery system after the monitor.

The associated values of radius at the workpiece (R_w) are given by:

$$R_w = R_m \left(\frac{F_w}{F_m}\right) \quad (6)$$

where R_m is the pinhole radius.

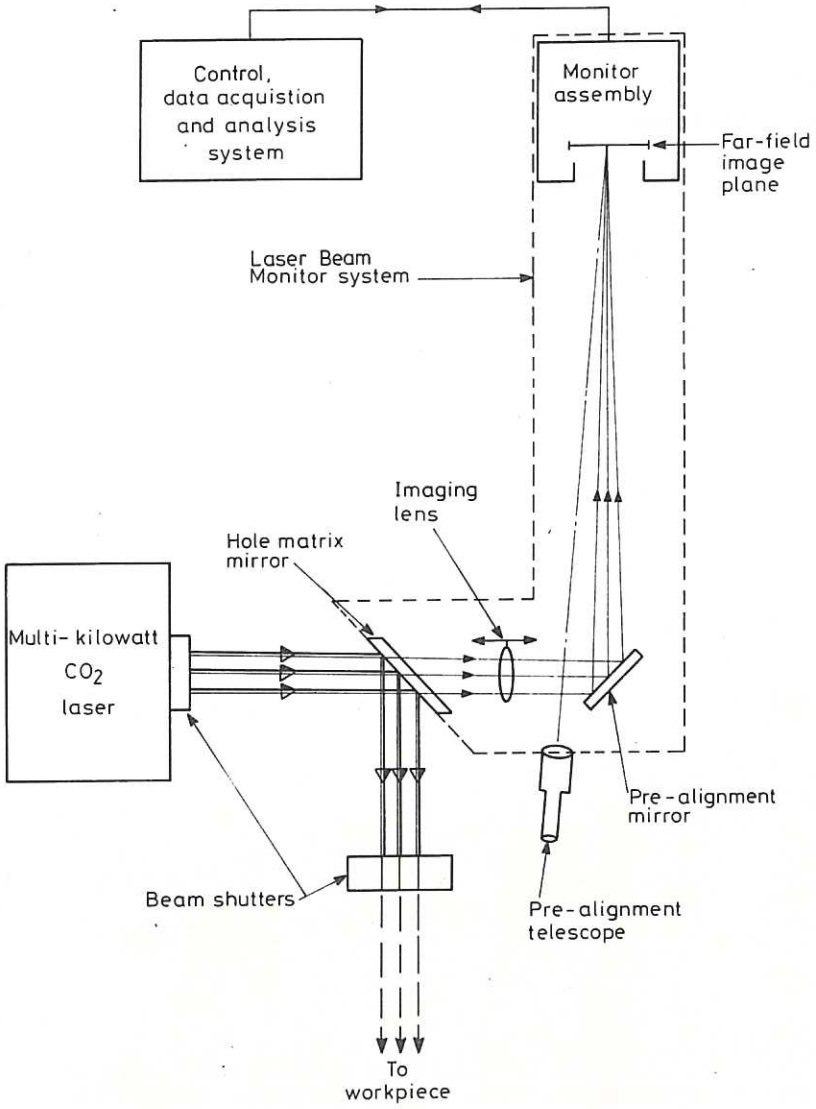

Fig 1 Schematic diagram of Laser Beam Monitor System and method of Insertion into Laser Beam Delivery Line

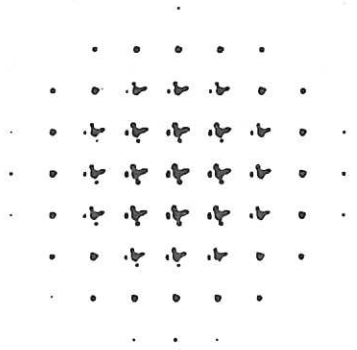

Fig 2 Burn Pattern in Acrylic Target of Far Field Image Matrix

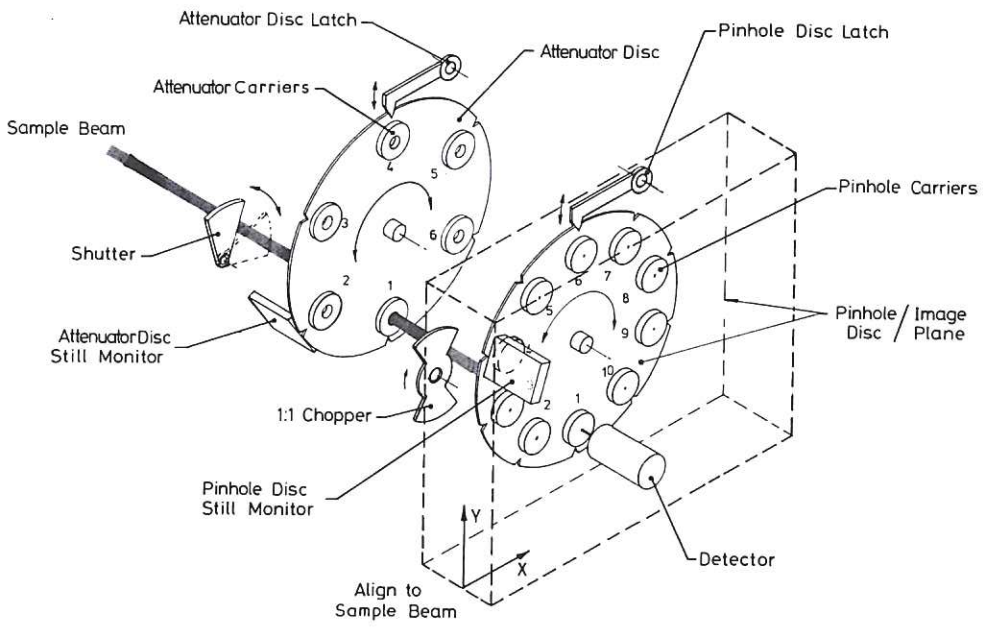

Fig 3 Schematic diagram of Monitor Assembly

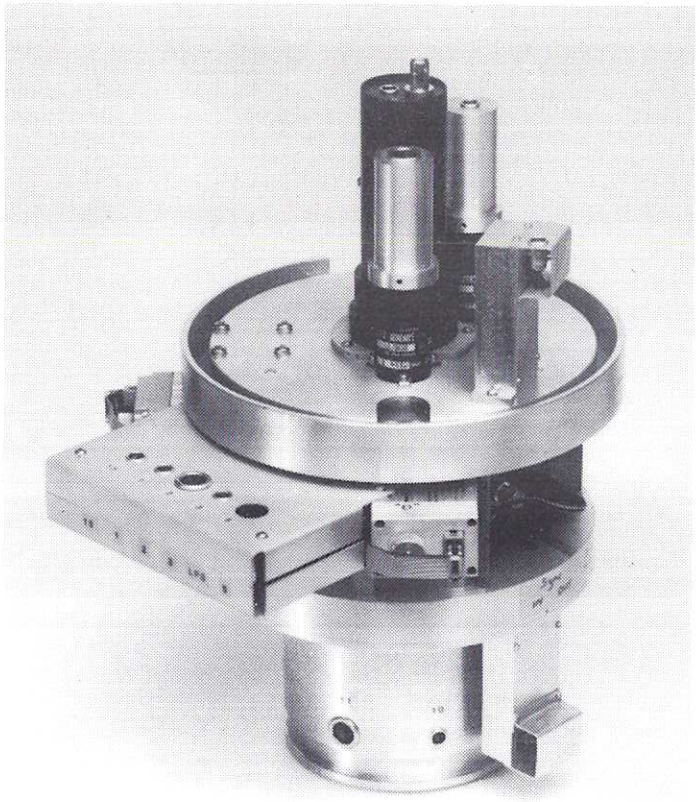

Fig 4 Monitor Assembly

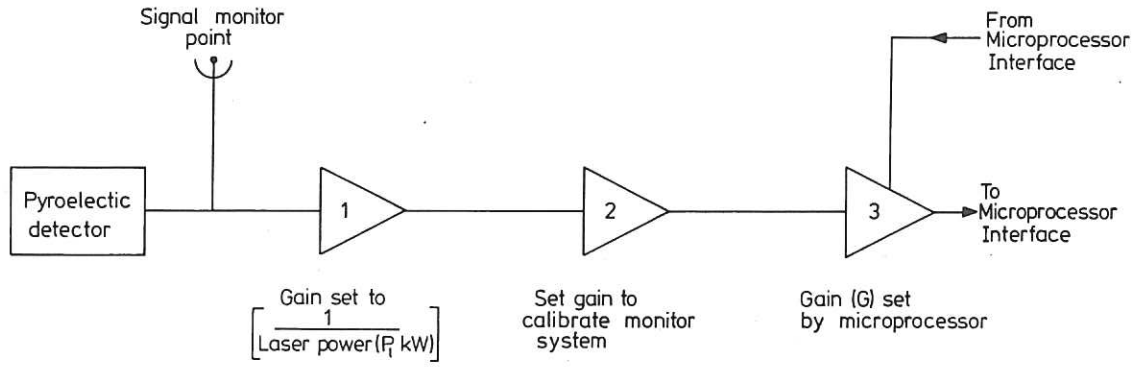

a) Pyroelectric Detector

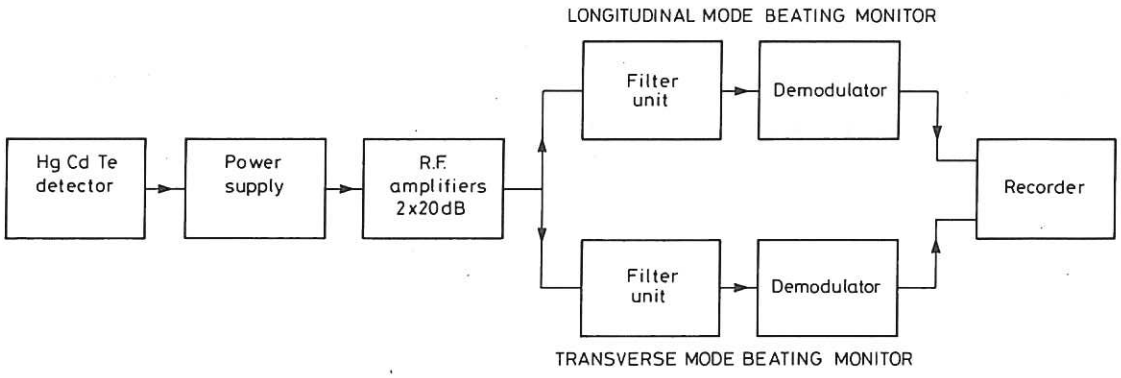

b) HgCdTe Detector

Fig 5 Schematic diagrams of Detector Electronics

PEAK POSN. (0, 0) CHANGE (0, 0)

DET. O/P 573, AMP GAIN IS 10, STEP SIZE 320

```
0 0 0 0 0 0 0 0 0 0 0 0
0 0 0 0 0 0 0 0 0 0 0 0
0 0 0 0 1 2 1 1 0 0 0
0 0 0 2 5 5 3 2 1 0 0
0 0 0 4 7 B 9 4 2 0 0
0 0 1 3 8 E C 5 2 0 0
0 0 1 3 5 9 9 5 2 0 0
0 0 1 1 2 3 3 3 1 0 0
0 0 0 1 1 1 1 1 0 0 0
0 0 0 0 0 0 0 0 0 0 0
0 0 0 0 0 0 0 0 0 0 0
```

a) Routine 1

100% TRANS. DETECTOR OUTPUT IS 1021

PINHOLE RADIUS (mm)	ATTENUATOR	PERCENTAGE TRANSMISSION	TRANSMISSION R.M.S.	AV. INTENS IN ANNULUS
1.60	NONE	100.0	1.5	-
0.15	NONE	5.7	8.2	834.6
0.30	NONE	15.4	6.3	466.8
0.50	NONE	32.4	6.8	344.1
0.75	NONE	70.2	4.6	393.1
1.00	NONE	85.8	2.5	116.4
1.25	NONE	95.7	1.1	57.1
1.50	NONE	99.1	1.4	15.7
1.60	NONE	100.0	1.3	-
1.60	POL. (90)	1.3	1.4	-
1.60	POL. (0)	83.9	1.4	-
1.60	CaF2	20.0	0.9	-
1.60	NONE	99.9	1.5	-

b) Routine 2

Fig 6 Output from Pyroelectric Detector Data Analysis Routines

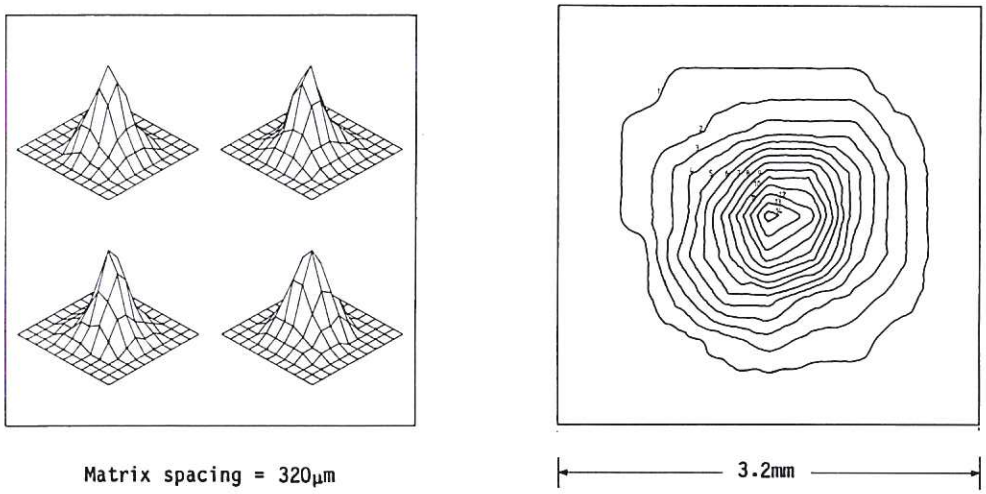

Fig 7 Additional representations of Output from Pyroelectric Detector Data Analysis Routine 1

Annulus radii (mm)		
	Min	Max
o	0	0·15
Δ	0·15	0·30
◇	0·30	0·50
x	0·50	0·75
□	0·75	1·00
+	1·00	1·25
0	1·25	1·50

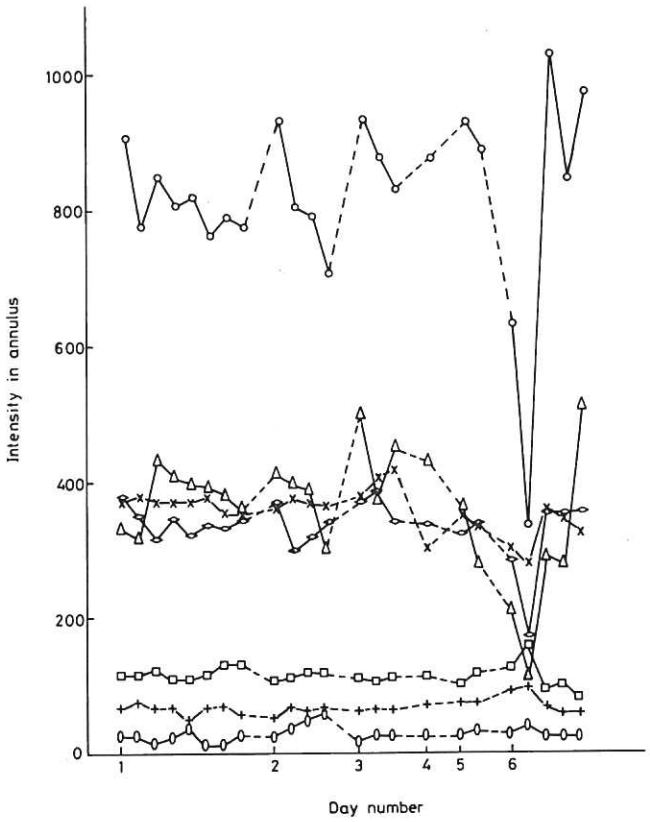

Fig 8 Time dependence of Far Field Intensity Profile of Fast Axial Flow 1kW laser

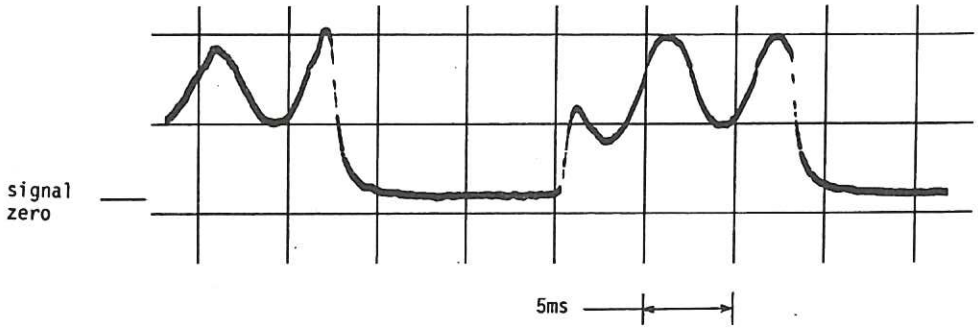

Pinhole diameter 0.3mm
Attenuator none

Fig 9 Chopped Pyroelectric Detector output signal showing variations associated with Laser Mode Instabilities

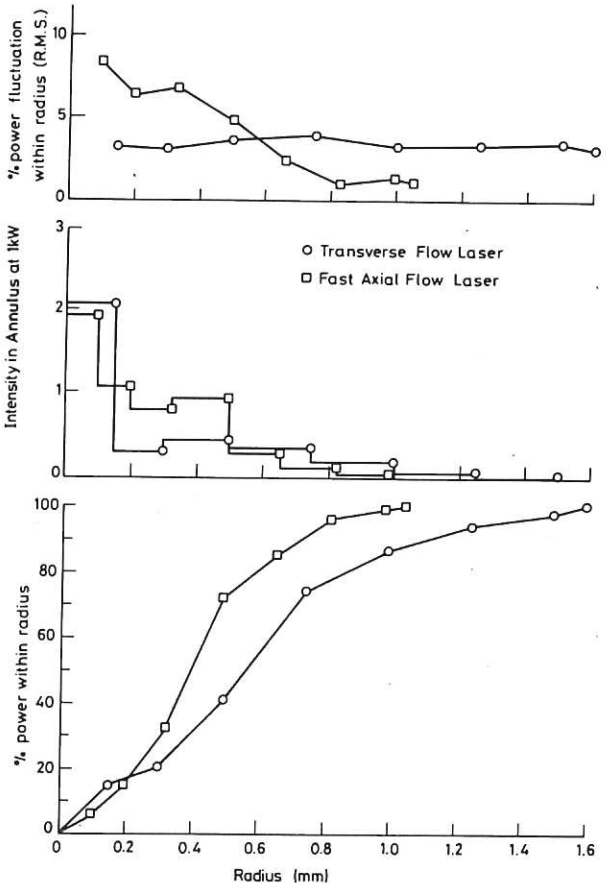

Imaging Lens optical aperture F/25

Fig 10 Comparisons of 1kW Fast Axial Flow and 5kW Transverse Flow Lasers

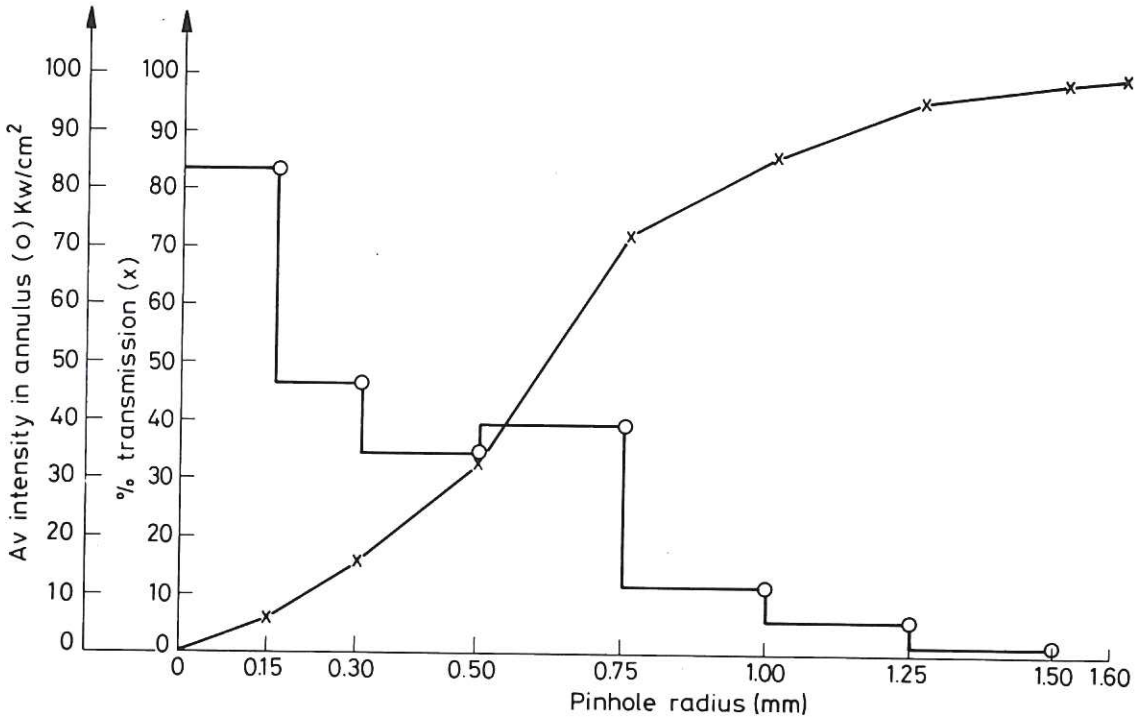

Imaging Lens optical aperture F/38 Laser Power 1kW

Fig 11 Beam Profile Data derived from Data Analysis Routine 2

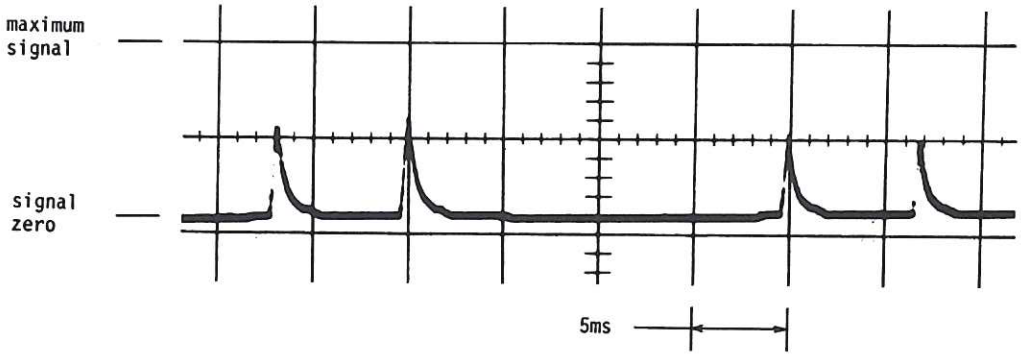

Pinhhole 3.2mm square
Attenuator Grid polariser (orientation 90°)

Fig 12 Chopped Pyroelectric Detector output signal showing variations associated with Polarization Instabilities

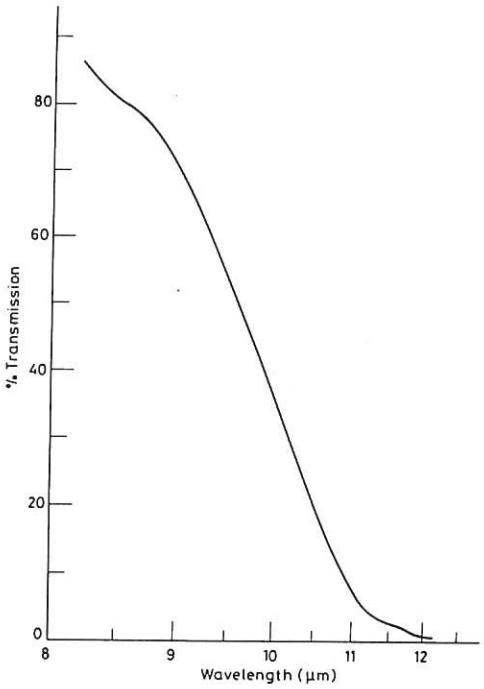

Fig 13 Wavelength dependence of Transmission through 4mm thick CaF_2

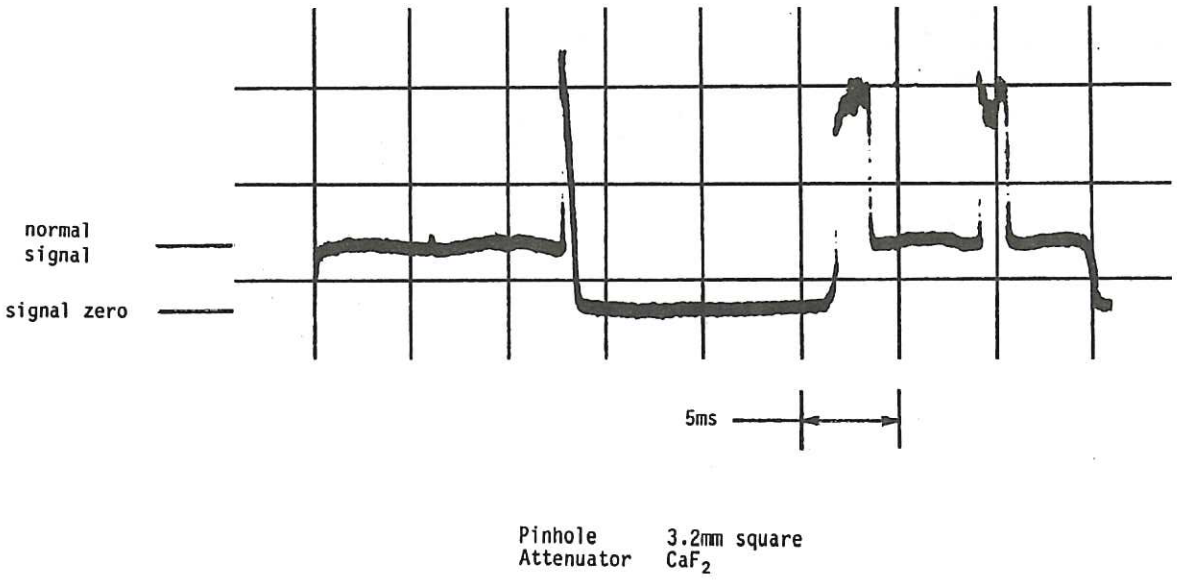

Fig 14 Chopped Pyroelectric Detector output signal showing increases in amplitude associated with decrease in Laser Output Wavelength

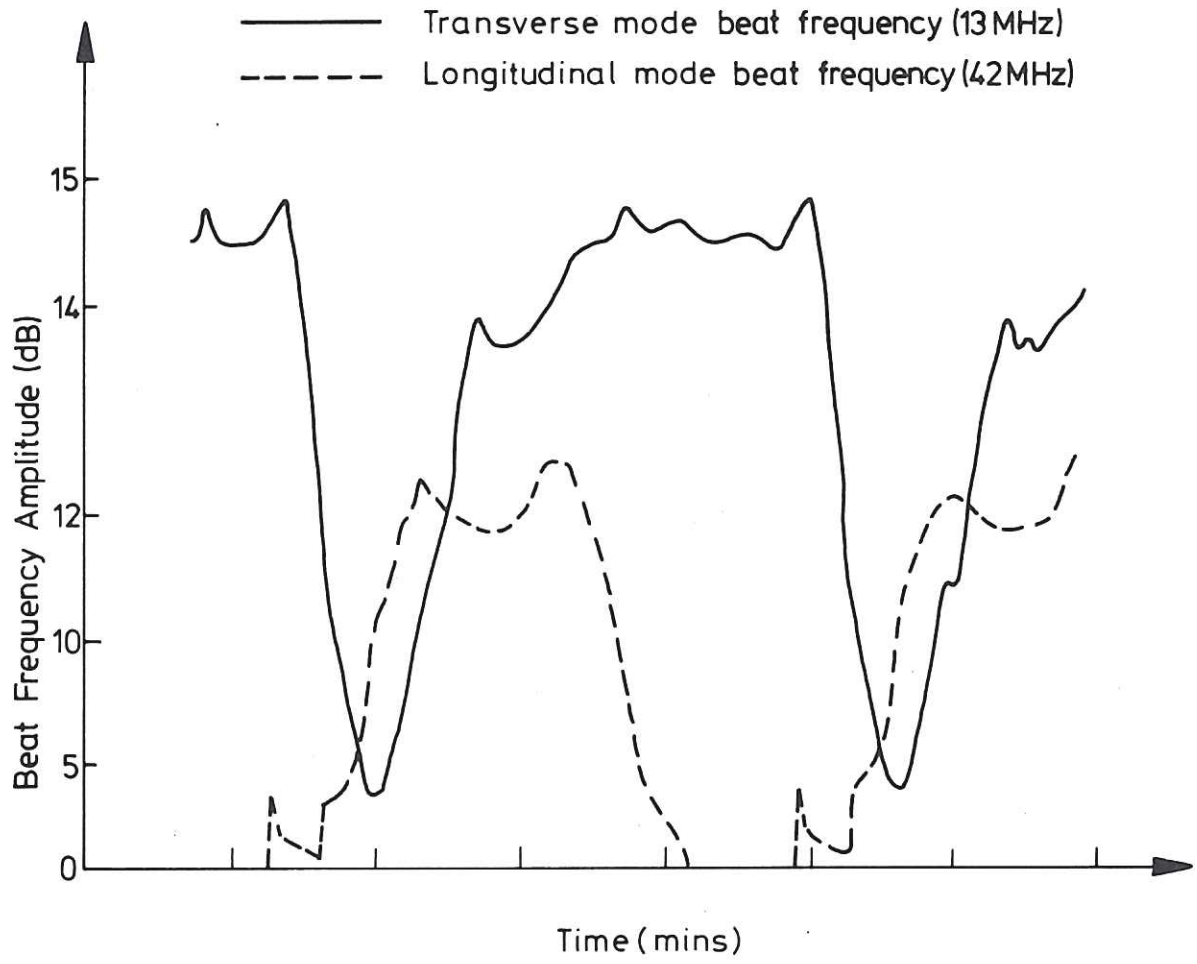

Fig 15 Amplitude of the beat frequencies associated with the Longitudinal and Transverse mode activity of a 1kW Fast Axial Flow Laser

Available from
HER MAJESTY'S STATIONERY OFFICE
49 High Holborn, London, WC1V 6HB
(Personal callers only)
P.O. Box 276, London, SE1 9NH
(Trade orders by post)
13a Castle Street, Edinburgh, EH2 3AR
41 The Hayes, Cardiff, CF1 1JW
Princess Street, Manchester, M60 8AS
Southey House, Wine Street, Bristol, BS1 2BQ
258 Broad Street, Birmingham, B1 2HE
80 Chichester Street, Belfast, BT1 4JY

PRINTED IN ENGLAND